Numerical modelling of induced seismicity considering metre-scale stress heterogeneity in a fault damage zone

Atsushi Sainoki
Kumamoto University, Kumamoto city, Japan

ABSTRACT: It is of paramount importance to gain a better understanding of induced seismicity taking place in deep underground for sustainable energy developments. Notwithstanding the effort made in the numerical simulation of induced seismicity, there is still a large gap between analysis results and field observations. The present study aims at simulating spatially and temporally distributed fault-slip events whilst considering metre-scale stress heterogeneity. The result indicates that the heterogeneous fault confining stress is crucial in the occurrence of fault-slip. The analysis of b-values computed from multiple seismic events simulated on the fault plane demonstrated that the b-value decreases with the reduction of the effective normal stress, showing consistency with the characteristic of induced seismicity in the field. This implies the possibility of applying the simulation method developed in this study to the risk evaluation for seismic hazards through the b-value analysis based on the advanced fault-slip modelling approach.

Keywords: Induced-seismicity, stress heterogeneity, b-value, dynamic analysis.

1 BACKGROUND

Due to the depletion of shallow ore deposits, mining depths have been increasing around the world, leading to ore extraction under unfavorable geological and stress conditions, thereby causing serious problems that need to be addressed for sustainable developments at great depths. Mining-induced seismicity is well recognized as one of such problems, and seismic waves released could inflict devastating damage to underground facilities and openings in an extensive area in an underground mine when entailing rockbursts. Furthermore, seismic events with large magnitudes can cause noticeable ground vibrations, which may raise public concern depending on the intensity. For these reasons, it is of importance to develop methods for estimating the risk and mitigating the damage.

For decades, numerical modelling techniques have been intensively employed to analyze the stress regime of underground geological structures and estimate the potential of seismicity, including the identification of highly stressed region and source parameters of seismic events. However, there is a great gap between numerical modelling results and those of in-situ seismic monitoring in that the number of seismic events simulated with numerical models is significantly less compared to that

detected with seismic monitoring systems (Sainoki and Mitri, 2014). Furthermore, for numerical modelling, it is quite challenging to estimate the risk of seismic events taking place in geological structures located away from active mining areas, where mining-induced stress change is negligible compared to that in the vicinity of underground openings, such as drifts and stopes.

These difficulties are strongly associated with the heterogeneous stress state dependent on physical and mechanical properties of rock masses. Especially, the stress state becomes significantly complex in geological structures, e.g., fault, dyke, and shear zone, making it difficult to quantify seismic source parameters and evaluate the risk. In fact, most of numerical simulations previously performed for the stress analysis of deep underground mines assume the overburden and horizontal pressures that monotonically increase with the depth. Recently, Sainoki et al. (2021) developed a numerical modelling method to simulate fracture network-induced complex, heterogeneous stress state in a fault damage zone with an equivalent continuum model in conjunction with a discrete fracture network. The present study employs the method to simulate multiple seismic events on a fault plane whilst considering the fracture network-induced meter-scale stress heterogeneity.

2 NUMERICAL MODEL CONSTRUCTION

2.1 Generation of discrete fracture network

The first step to construct a numerical model is the generation of fracture network in a fault damage zone surrounding a fault core as shown in Figure 1(a). The present study refers to the comprehensive literature review on fracture characteristics in a fault damage zone provided by Sainoki et al. (2021). According to the review, a power law function was employed to reproduce the fracture density decay from a fault core to host rock, assuming 30/m as the maximum fracture density (P10) near the core. Regarding fracture orientation, the distribution is determined with Fisher distribution (Fisher, 1996) with the assumption that the mean dip angle and dip direction of fractures coincide with those of the fault. As for the fracture size, the maximum and minimum fracture sizes considered in the present study is 10 m and 2 m, respectively. It is to be noted that this study focuses on meter-scale stress heterogeneity. In this regard, the minimum fracture size is deemed sufficient as the stress state is insusceptible to centi- and milli-scale fractures on the scale of interest.

2.2 Equivalent continuum model based on the crack tensor theory

The discrete fracture network generated is then used to obtain equivalent compliance matrices based on the crack tensor theory (Oda, 1986). The crack tensor theory is described with the following equations.

$$\mathbf{F}_{ij} = \frac{1}{V}\frac{\pi}{4}D^3\mathbf{n}_i\mathbf{n}_j \tag{1}$$

$$\mathbf{F}_{ijkl} = \frac{1}{V}\frac{\pi}{4}D^3\mathbf{n}_i\mathbf{n}_j\mathbf{n}_k\mathbf{n}_l \tag{2}$$

$$\mathbf{C}_{ijkl} = \sum_{1}^{NCR}\left[\frac{1}{K_nD} - \frac{1}{K_sD}\right]\mathbf{F}_{ijkl} + \frac{1}{4K_sD}\left(\delta_{ik}\mathbf{F}_{jl} + \delta_{jk}\mathbf{F}_{il} + \delta_{il}\mathbf{F}_{jk} + \delta_{jl}\mathbf{F}_{ik}\right) \tag{3}$$

$$\mathbf{T}_{ijkl} = \mathbf{C}_{ijkl} + \mathbf{M}_{ijkl} \tag{4}$$

where **F** and **n** are the crack tensor and the unit normal vector of the fracture intersecting with the zone, respectively; **C**, **M**, and **T** represent the anisotropic compliance tensor equivalent to the elasticity of fractures, the isotropic compliance tensor of the rock mass, and the anisotropic compliance tensor of fault damage zone, respectively; *NCR* is the total number of fractures intersecting with the zone; K_n and K_s are shear and normal stiffnesses of the fracture, respectively; δ is the Kronecker's delta; and D denotes the diameter of the fracture.

The compliance tensor of each element in a continuum model constructed in the framework of the finite difference method is calculated with Equations (1) to (4). That is, each element has a different compliance matrix considering fracture network-induced anisotropic elasticity and stiffness heterogeneity.

2.3 Numerical model constructed

Figure 2(b) shows a perspective view of the continuum model generated in the combination of the discrete fracture network and the crack tensor theory. At the center of the model is a fault core running parallel to the *y*-*z* plane. The gray-colored zones in Figure 2(b) are those not including fractures, so that isotropic elasticity is assumed with the modulus of elasticity corresponding to that of the host rock, whilst elastic compliance matrices of the red-colored zones are computed based on the crack tensor theory. Figure 2(c) illustrates interface elements, which represent the fault core, to simulate fault-slip.

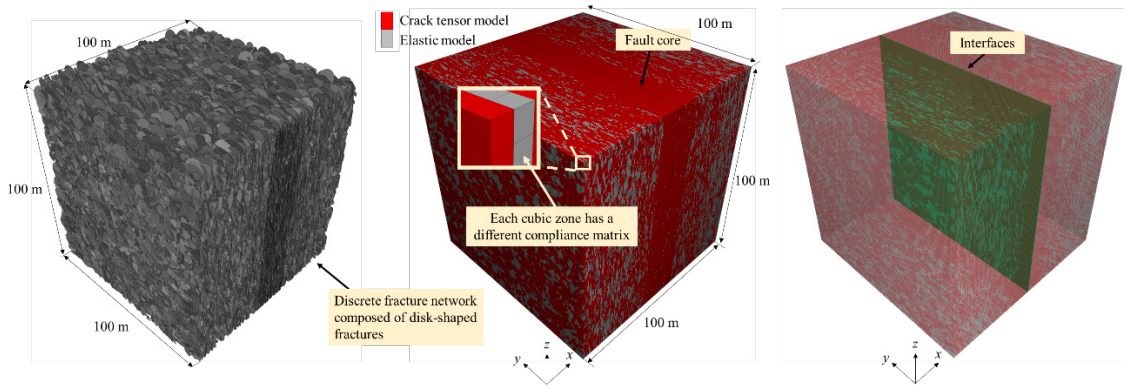

Figure 2. Model construction procedure: (a) discrete fracture network, (b) equivalent continuum model, (c) fault plane modelling with interface elements.

3 NUMERICAL MODEL SETTINGS

3.1 Mechanical properties of the rock mass and fault

Mechanical properties of the model are determined whilst assuming that the host rock is predominantly composed of granite. Accordingly, its elastic modulus and Poisson's ratio are set at 40 GPa and 0.2, respectively, considering the effect of fractures with lengths less than 2 m (Sainoki et al. 2021). As for the fractures, its normal and shear stiffnesses are set at 30 GPa/m and 10 GPa/m (Eftekhari et al. 2014), which are used in Equation (3). Regarding the interface element to model the fault core, its normal and shear stiffnesses are assumed to be 1.0 GPa/m and 0.3 GPa/m, respectively, considering the difference in scale between the fault plane and fractures in the fault damage zone. The friction angle of the fault is set at 30º (Barton 1976). The cohesion is assumed to be zero. To simulate fault-slip, the Coulomb's shear strength model with a slip-weakening law is employed. That is, when the shear stress acting on the fault exceeds the shear strength determined by the failure criterion, the friction angle is instantaneously decreased from 30° to 20°.

3.2 Analysis procedure

First, static analysis is performed to simulate an initial stress state whilst applying gravity force and boundary tractions. It is to be noted that the direction of gravity is rotated at 20° in anticlockwise direction to simulate a fault with a dip angle of 70°. Accordingly, the tractions applied to the model outer boundaries is asymmetric as shown in Figure 3(a).

Then, the effective normal stress of the fault plane is decreased in the circular region of the fault to induce fault-slip, as depicted in Figure 3(b). The reduction of the effective normal stress assumes general anthropogenic activities at great depths, such as a large amount of ore extraction and fluid injection. Assuming hydrostatic pore pressure as an initial condition, the effective normal stress is decreased by 0.5 MPa in a stepwise manner. At each stage, the initiation of non-linear shear movement is investigated on the fault plane. Then, when slip is detected, the analysis condition is changed from static to dynamic in order to simulate fault-slip in a dynamic condition. At that time, the boundary condition is changed to viscous boundary. After the dynamic slip is ceased, the analysis condition returns to static, and subsequently the effective stress is repeatedly decreased.

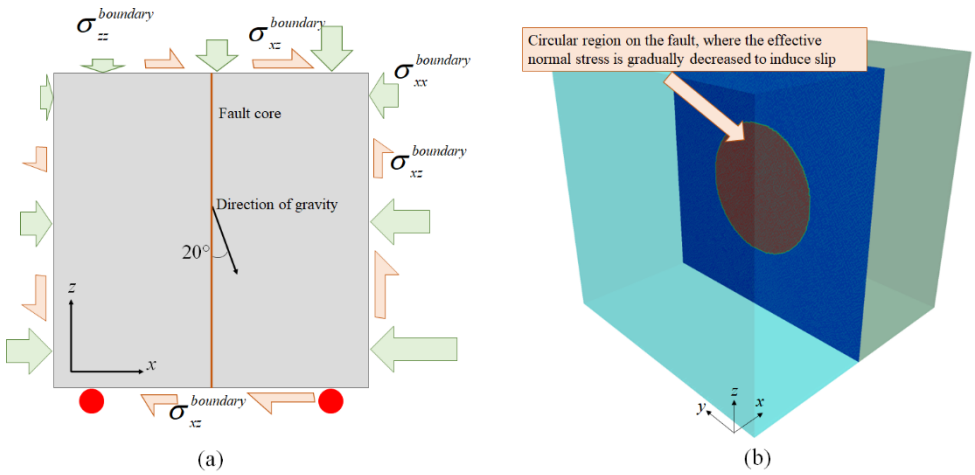

Figure 3. Analysis conditions: (a) boundary condition to calculate initial stress state, (b) circular region on the fault plane to simulate fault slip with the reduction in effective normal stress.

4 RESULTS AND DISCUSSIONS

4.1 Initial stress state of the fault before reducing the effective normal stress

Figure 5 illustrates the stress state on the fault plane in the circular region before simulating fault-slip in dynamic conditions. It is remarkable that the stress state is significantly complex and heterogeneous, affected by the meter-scale stiffness heterogeneity of the surrounding rock mass and its anisotropy, generating local regions with high stresses for both normal and shear stresses. Interestingly, the fault patches with high normal stresses do not coincide with those with high shear stresses. This implies that some patches may have large fault-slip potential on the initial stress state, given that there exist fault patches with low normal stress and high shear stresses on the fault plane. Figure 5(c) shows effective stress change required to initiate fault-slip on the fault plane, which is calculated from the stresses in Figure 5(a) and (b). As can be seen, there are large variations ranging from almost 0 MPa to 27 MPa, i.e., for patches with cool colors a slight change in the effective normal stress could cause fault-slip.

Figure 6 shows the relative frequency of the stresses shown in Figure 5. The result indicates that the deviation of normal stress is much larger than that of the shear stress, corresponding to the large variation of the effective stress in Figure 6(c). These results indicate that the normal stress variation plays a crucial role in the occurrence of fault-slip.

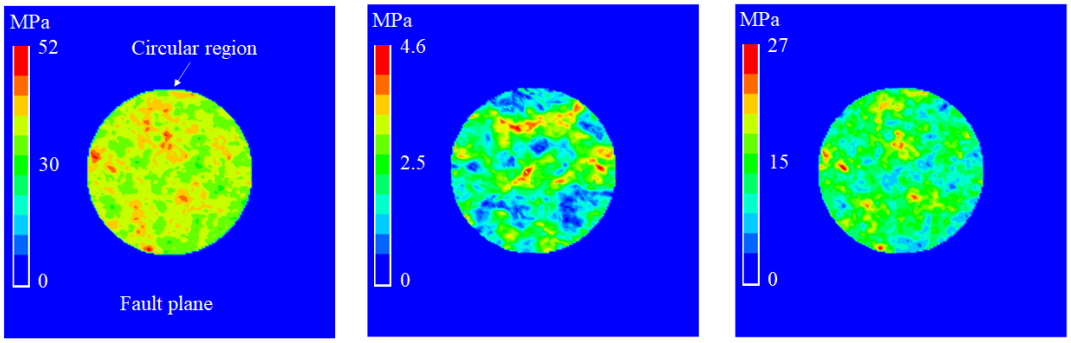

(a) (b) (c)

Figure 5. Stress state in the circular region on the fault plane: (a) normal stress, (b) shear stress, (c) effective stress change required to initiate fault-slip.

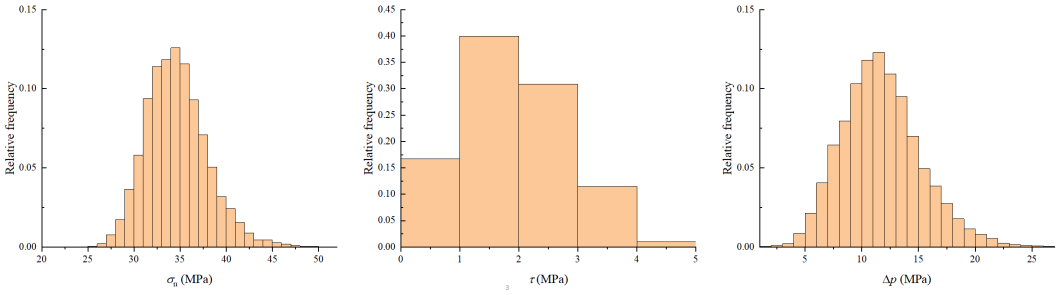

(a) (b) (c)

Figure 6. Stress distribution in the circular region: (a) normal stress, (b) shear stress, (c) effective stress change required to initiate fault-slip.

4.2 Distribution of seismic events and b-value analysis

Figure 7 depicts dynamic fault-slip events that took place during the sequential effective pressure reduction. As each seismic event is composed of multiple fault patches, seismic events are distinguished with different colors. It is found from the figures that the number of seismic events obviously increases with the decrease in the effective stress on the fault plane and that a larger area tends to slip for each seismic event at later stages. Hence, it can be concluded that the effective stress reduction leads to the increase in the frequency and intensity of fault-slip events.

To make a quantitative evaluation regarding the variation of magnitude between early and later stages, b-value was computed for each stage, and the result is summarized in Figure 8. As shown, b-value decreases from 1.67 to 0.76 with the reduction of the effective stress, implying the increase in the frequency of relatively large events. Remarkably, this tendency agrees well with field observations of induced seismicity in deep underground mines, i.e., the presented method is capable of reproducing characteristics of induced seismicity in deep underground to some extent.

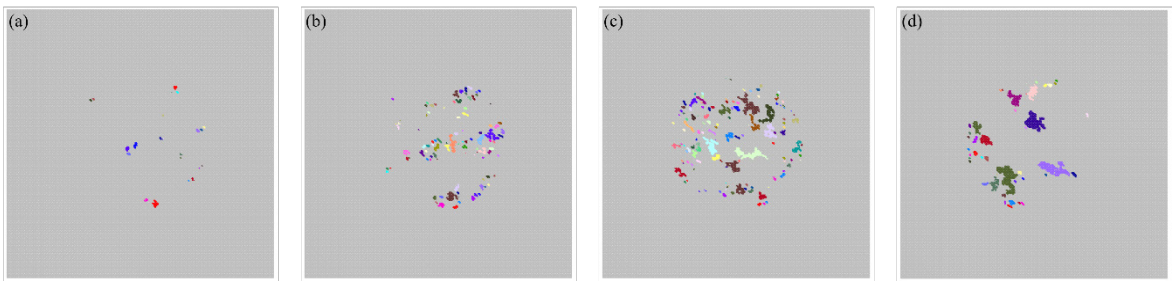

Figure 7. Simulated seismic events: (a) 10th stage, (b) 15th stage, (c) 20th stage, (d) 25th stage.

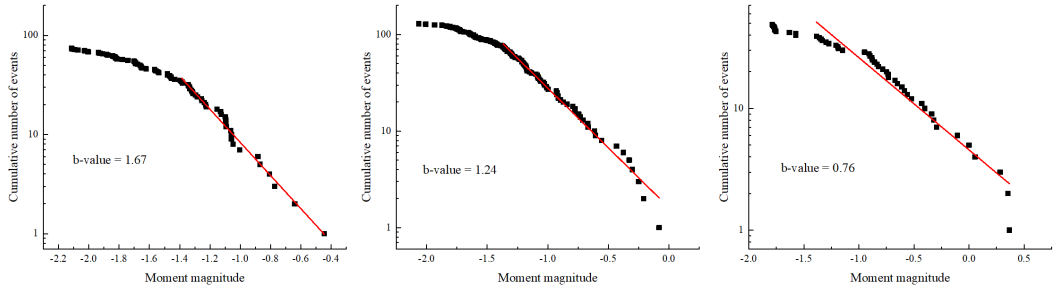

Figure 8. b-values computed for different stages: (a) 15th stage, (b) 20th stage, (c) 25th stage.

5 CONCLUSION

The present study simulates induced seismicity taking place on a fault plane whilst considering its complex stress state resulting from the fracture network-induced metre-scale stiffness heterogeneity in a fault damage zone. The result indicates that the heterogeneity of fault confining stress is crucial in the occurrence of fault-slip rather than the shear stress. The characteristic of multiple seismic events simulated on the fault plane was analyzed in terms of b-value, and it was demonstrated that b-value decreases from 1.67 to 0.76 with the reduction of the effective normal stress, indicating consistency with the characteristic of induced seismicity observed in the field. This suggests the possibility of applying the simulation method developed in this study to the risk evaluation of seismic hazards by computing b-values obtained from the numerical model producing spatially and temporally distributed seismic events on a fault plane.

ACKNOWLEDGEMENTS

The present study was supported by KAKENHI 19K15493.

REFERENCES

Barton, N. 1976. Rock mechanics review the shear strength of rock and rock joints. International Journal of Rock Mechanics and Mining Science Geomechanics Abstract 13, pp. 255-279.

Eftekhari, M., Baghbanan, A. & Bagherpour, R. 2014. The effect of fracture patterns on penetration rate of TBM in fractured rock mass using probabilistic numerical approach. Arabian Journal of Geosciences (7), pp. 5321–5331.

Fisher, N.I. 1996. Statistical analysis of circular data *Cambridge University Press*.

Oda, M. 1986. An equivalent continuum model for coupled stress and fluid flow analysis in jointed rock masses. Water Resources Research 22(13), pp. 1845-1856.

Sainoki, A. & Mitri, H.S. 2014. Methodology for the interpretation of fault-slip seismicity in a weak shear zone. Journal of Applied Geophysics 110, pp. 126-134.

Sainoki, A., Schwartzkopff, A.K., Jiang, L. & Mitri, H.S. 2021. Numerical Modeling of Complex Stress State in a Fault Damage Zone and Its Implication on Near-Fault Seismic Activity. Journal of Geophysical Research: Solid Earth 126 (7), e2021JB021784.